J Mater Sci: Mater Med (2010) 21:695–705
DOI 10.1007/s10856-009-3920-0

Physico-chemical and in vitro biological evaluation of strontium/calcium silicophosphate glass

Saeed Hesaraki · Masoud Alizadeh · Hamid Nazarian · Davood Sharifi

Received: 23 May 2009 / Accepted: 19 October 2009 / Published online: 29 October 2009

Abstract Strontium is known to reduce bone resorption and stimulate bone formation. Incorporation of strontium into calcium phosphate bioceramics has been widely reported. In this work, calcium and calcium/strontium silicophosphate glasses were synthesized from the sol–gel process and their rheological, thermal, and in vitro biological properties were studied and compared to each other. The results showed that the gel viscosity and thus the rate of gel formation increased by using strontium in glass composition and by increasing aging temperature. In strontium-containing glass, the crystallization temperature increased and the type of the crystallized phase was different to that of strontium-free glass. Both glasses favored precipitation of calcium phosphate layer when they were soaked in simulated body fluid; however strontium seemed to retard the rate of precipitation slightly. The in vitro biodegradation rate of the strontium/calcium silicophosphate glass was higher than that of strontium-free one. The cell culture experiments carried out using rat calvaria osteoblasts showed that the incorporation of strontium into the glass composition stimulated proliferation of the cells and enhanced their alkaline phosphatase activity, depending on cell culture period.

S. Hesaraki (✉) · M. Alizadeh
Ceramics Department, Materials and Energy Research Center, Tehran, Iran
e-mail: s-hesaraki@merc.ac.ir

H. Nazarian
Royan Institue, Tehran, Iran

D. Sharifi
Department of Clinical Science, Surgery and Radiology, Faculty of Veterinary Medicine, University of Tehran, Tehran, Iran

1 Introduction

Bioceramics such as calcium phosphates and bioglasses have been extensively used in the treatment of bone defect, osteoporotic problems and elderly patients with lower osteogenesis [1].

Bioactive glasses are important group of materials with a wide range of application in medicine as bone substitute. These materials are able to bind with bone in a living organism through a layer of hydroxyapatite (HA) formed on their surfaces [2].

Bioactive glasses can be obtained by melting a dried batch of starting materials at elevated temperatures or by a low temperature process known sol–gel [3].

Based on the earlier work of Hench and co-workers, sol–gel method can produce high purity glasses with higher homogeneity, higher surface area and porosity, and more bioactivity in comparison with melt-derived glasses [4]. Furthermore, bioactivity in melt-derived glasses is limited to a compositional range and SiO_2 must be lower than 60 mol%, while a bioactive glass prepared from the sol–gel process may be composed of 100% SiO_2 [5].

There is a constant need for bone implant formulations such as bioglasses that have better osseointegrative properties. One of the approaches to improve bone stimulating properties of these biomaterials is incorporation of bone stimulator ions into their chemical compositions [6].

Many researches have focused on preparation and characterization of bioceramic-based biomaterials, whether crystalline bioceramics or amorphous bioglasses, incorporated with some ions such as Zn, Mg and Si because of their unique effect on osteoblastic cell proliferation, differentiation and thus bone mineralization [7–10].

Strontium (Sr) is another ion known to reduce bone resorption and accelerate bone healing processes [11].

In vitro and in vivo studies have indicated that strontium increases bone formation and reduces osteoprosis, leading to a gain in bone mass and improved bone mechanical properties in normal animals and humans [12–16]. Consequently, several studies have been also conducted on the use of Sr ions in the composition of bioceramic-based biomaterials. For example, Landi et al. [17] synthesized Sr-substituted hydroxyapatite and studied its mechanical, physico-chemical and structural properties. There are however limited studies on strontium-containing bioactive glass bone substitutes. The role of Sr on the structure and reactivity of dental ionomer glasses has been reported by Boyd et al. [18]. Abou Neel et al. [19] reported some structural and physical characteristics of melt-derived phosphate glasses based on Na_2O–CaO–SrO–P_2O_5 system. Both in vitro and in vivo reactivity of a melt-derived bioglass system based on SrO–CaO–ZnO–SiO_2 were also evaluated by Towler et al. [20] and it was found from their results that the glass is incapable of forming an apatite layer in simulated body fluid (SBF).

The objective of the present study was to produce a sol–gel derived bioactive silicophosphate glass based on SiO_2–CaO–SrO–P_2O_5 system and compared its physico-chemical, bioactivity and cellular properties to those of a Sr-free bioactive glass using proper analytical techniques. In this paper the vocabularies Sr-glass, Sr glass and Sr-containing glass are synonyms.

2 Materials and methods

2.1 Synthesis and characterization of glasses

Table 1 presents chemical composition of the glasses along with the code of each composition used in this study. The following precursors were used for the synthesis of the glasses: Tetraethylorthosilicate (TEOS), triethylphosphate (TEP), calcium nitrate tetrahydrate and strontium nitrate. All precursors were purchased from the Merck Company. Aqueous solution of the gel was prepared using stoichiometric amounts of each precursor and the gels were obtained as the method described previously [7]. Briefly, TEOS was poured into 0.1 M nitric acid solution and stirred for 1 h at room temperature for acid hydrolysis. Then TEP, calcium nitrate and strontium nitrate (if necessary) were added to the TEOS solution in sequence allowing 45 min for each reagent to react completely. Then, the mixture was stirred for 1 h for completion of the hydrolysis reaction. The solution was poured into Teflon container, kept sealed at 25°C for 6 days, dried at 70°C for 3 days and 120°C for 2 days, and finally heated at 800°C for 3 h to eliminate the residual nitrate and organic substances.

Table 1 Chemical composition of the glasses studied in this work (in wt%)

Glass code	CaO	SrO	SiO_2	P_2O_5
Sr-free glass	27.6	0	61.1	11.3
Sr glass	22.3	7.9	58.8	11.0

To evaluate the effect of temperature on gelling behavior of different sols, the sols were prepared by the same method described above but aged at two different temperatures: 25 and 37°C. Then, the samples were taken at various intervals during the condensation process and their viscosity was recorded using Brookfield cone-plate viscometer (model DV-II), at a constant shear rate of 750 s^{-1}, based on the previously described method [21].

Powder density of the samples (ρ) was also measured using a gas picnometer device (Micrometrics Accupy C 1330). To determine proper heating temperature for the removal of residual organic and nitrate precursors without any crystallization, thermal behavior of dried gels were carried out up to 1200°C. For this purpose the powdered gel was heated up to 1200°C, at heating rate of 5°C/min, using a PL-STA 1600 instrument (England). Powdered alumina was used as reference material. To identify phase composition of the crystallized glasses, the samples were heated at 1000°C for 2 h.

2.2 In vitro bioactivity test

The in vitro bioactivity of the glasses was conducted on disc-shaped samples (10 mm in diameter and 0.3 mm in height) formed by pressing the glass powder in hydraulic press device at 9 MPa followed by heating at 800°C. Then the samples were soaked in simulated body fluid (SBF) at 37°C for various periods up to 14 days. The SBF solution was prepared by Kokubo's specification [22], i.e., dissolving NaCl, KCl, K2HPO_4, 3H_2O, $MgCl_2$·6H_2O, $CaCl_2$, and Na_2SO_4 reagents in distilled water and buffering the solution with tris(hydroxymethyl) amminomethane ($(HOCH_2)_3CNH_2$). The pH of the solution was adjusted at 7.4 using hydrochloric acid. All chemical reagents used for preparation of the SBF were extra pure grade (>99%) and purchased from the Merck company (Germany). At the end of each day, whole of the solution was extracted to estimate its Ca and Si concentration by inductively coupled plasma (ICP-AES) technique and immediately fed by fresh SBF solution.

Phase composition of the samples was checked by X-ray diffractometry (XRD), at 1 and 2 weeks after soaking in SBF. The patterns of unsoaked glass specimens were also taken for comparison. For this purpose, the samples were removed from the SBF, washed with distilled water, dried

at room temperature, ground to fine powder and analyzed using a Philips PW3710 X-ray diffractometer with Ni filter and Cu target. The patterns were identified by JCPDS-International Center for Diffraction Data Cards.

The chemical groups in glasses were examined by Fourier transform infrared (FTIR) analysis. Fine powders of specimens were mixed with KBr powder by the ratio of 1:100 and transparent homogenous discs were formed by pressing the mixture under 5 ton/cm^2 pressure. In this test, data were collected at room temperature at the wavenumber range of 4000–400 cm^{-1} using a spectrometer Bruker Vector 33.

The surface morphologies of the specimens were analyzed by scanning electron microscope (SEM, Stereoscan S 360, Cambridge), at operating voltage of 20 kV and current intensity of 10 mA. Because of the poor electrical conductivity of the samples, their surfaces were coated with a thin layer of gold before the test.

2.3 Osteoblasts proliferation and morphologies on the bioglass specimens

To evaluate biological properties of the glasses, osteoblastic cells were derived from newborn rat calvaria and isolated by sequential collagenase digestion from calvaria of newborn (2–5 days) Wistar and cultured in Dulbecco modified Eagle medium (DMEM; Gibco-BRL, Life Technologies, Grand Island, NY) supplemented with 15% fetal bovine serum (FBS; Dainippon Pharmaceutical, Osaka, Japan) and 100 g/ml penicillin–streptomycin (Gibco-BRL, Life Technologies) in 5% CO_2 and 95% air atmosphere at 37°C for 1 week. The medium was changed every 2 days. The confluent cells were dissociated with trypsin and subcultured to three passages which were used for tests.

Proliferation study was performed to investigate the biofunctionality of the materials.

The disc-shaped bioglass specimens (6 mm in diameter and 3 mm in height) were sterilized using 70% ethanol and the osteoblastic cells were seeded onto the tops of the glass discs at 2×10^4 cells/disc. Polystyrene discs with diameter of 6 mm (the same surface area compared to glass specimens) were prepared from the tissue culture plate and similarly were seeded with the cells as control specimens. The specimen/cell constructs were placed into 24-wells culture plates and left undisturbed in an incubator for 3 h to allow the cells to attach to them and then an additional 3 ml of culture medium was added into each well. The cell/specimen constructs were cultured in a humidified incubator at 37°C with 95% air and 5% CO_2 for 1, 3, and 7 days. The medium was changed every 3 days.

The proliferation of the osteoblastic cells on bioglass and control specimens was determined using the MTT (3-{4,5-dimethylthiazol-2yl}-2,5-diphenyl-2H-tetrazolium bromide) assay. For this purpose, at the end of each evaluating period, the medium was removed and 2 ml of MTT solution was added to each well. Following incubation at 37°C for 4 h in a fully humidified atmosphere at 5% CO_2 in air, MTT was taken up by active cells and reduced in the mitochondria to insoluble purple formazan granules. Subsequently, the medium was discarded and the precipitated formazan was dissolved in dimethylsulfoxide, DMSO, (150 ml/well), and optical density of the solution was read using a microplate spectrophotometer (BIO-TEK Elx 800, Highland park, USA) at a wavelength of 570 nm.

To observe the morphologies of the cells attached onto the surfaces of the glass specimens, the cells were cultured onto the glass discs as described above. After 7 days, the culture medium was removed, the cell-cultured specimens were rinsed with phosphate buffered saline (PBS) twice and then the cells were fixed with 500 ml/well of 3% glutaraldehyde solution (diluted from 50% glutaraldehyde solution (Electron Microscopy Science, USA) with PBS). After 30 min, they were rinsed again and kept in PBS at 4°C. Specimens were then fixed with 1% Osmium tetroxide (Polyscience, Warmington, PA, USA). After cell fixation, the specimens were dehydrated in ethanol solutions of varying concentration (30, 50, 70, 90, and 100%) for about 20 min at each concentration. The specimens were then dried in air, coated with gold and analyzed by SEM (Streoscan S 360, Cambridge).

2.4 Alkaline phosphatase activity

The osteoblastic cells were seeded on the disc specimens under the same culturing conditions described above and the level of alkaline phosphatase activity (ALP) activity was determined on days 2, 5 and 7. Cells were rinsed twice with phosphatase buffered saline (PBS) followed by trypsinization and then scraped into double-distilled water. The cell lysates were frozen and thawed three times to disrupt the cell membranes. ALP activity was measured at 405 nm using p-nitrophenyl phosphate (pNPP) (Sigma, USA) as the substrate. A 50 ml sample was mixed with 50 ml pNPP (1 mg/ml) in 1 M diethanolamine buffer containing 0.5 mM $MgCl_2$, pH 9.8 and incubated at 37°C for 30 min on a bench shaker. The reaction was stopped by the addition of 50 ml of 1 N NaOH. Total protein content was determined using Coomassie brilliant blue method as described elsewhere [23]. The ALP activity was expressed as unit per mg protein.

2.5 Statistical analysis

Quantitative data were presented as means ± standard deviation (SD) of at least four experiments. Statistical

analysis was assessed using SPSS (v10.0). A student's *t*-test (assuming equal variances) was performed to determine the statistical significance between experimental groups. A probability value lower than 0.05 was considered to be statistically significant.

3 Results and discussion

3.1 Characterization of the glasses

In the present work, the preparation, in vitro characterization and biocompatibility of two different sol–gel derived bioactive glasses have been described. In chemical composition of one samples SrO was used because of its stimulating role in bone metabolism and cell proliferation. Some author [24] reported reduced biocompatibility of bioceramics incorporated with high doses of Sr thus, in this study low concentration of SrO was formulated in the glass composition (7.9 wt% equal to 5 mol%).

The powder density of Sr-containing glass was 2.651 ± 0.004 g/cm^3, a value that was significantly higher than that of Sr-free glass i.e., 2.674 ± 0.002 g/cm^3 ($P = 0.03$). It is originated from difference in theoretical density of SrO (4.7 g/cm^3) and CaO (3.4 g/cm^3).

Figure 1 shows the viscosity of the sols of various glasses during the aging process at 25°C (Fig. 1a) and 37°C (Fig. 1b). Viscosity of the sols was low during the most of aging time but increased suddenly at a certain time. The increase in viscosity of the sols is correlated to condensation process led to formation of chains by the colloidal sols, their growth, crosslinking and thus formation of network structure called gel. As observed in Fig. 1, the rate of condensation and gel formation increased by increasing the aging temperature and by incorporating SrO into the glass composition. A possible explanation to describe this phenomenon might be found in higher reactivity of SrO in comparison with CaO. Sr is less electronegative than Ca. Compared to elements with higher electronegativity, elements with lower electronegativity tend to form oxides with higher basicity and reactivity [18].

Figure 2 represents simultaneous thermal analysis (STA) patterns of bioglass specimens as thermal gravimetry (TG) and differential thermal analysis (DTA) (Fig. 2a for Sr-free glass and Fig. 2b for Sr-containing glass). In DTA patterns of both Sr-free and Sr-containing sample, the exothermic peak appeared around 150°C and accomplished with a mass loss of 25 wt% was attributed to removal of chemically adsorbed water. The peaks observed at 540–570°C and 580–650°C temperature ranges arose from condensation of silanol groups and removal of nitrates, respectively. These peaks are accomplished with a weight loss of about 18% in both specimens. Total weight loss of about 43% occurred during heating the specimens up to 1200°C. The STA patterns confirmed that the residuals could be removed at temperature below 650°C. According to Fig. 2a, the exothermic peak observed at 870°C was corresponded to glass devitrification phenomenon, which occurred at 905°C in Sr-containing specimen. The shift in crystallization temperature of Sr-glass can be correlated with its increased density and the nature (type) of the crystallized phase. To clarify this suggestion, the stabilized glass powders were heat treated at 1000°C for 2 h.

Figure 3 shows the X-ray diffraction patterns of sol–gel derived glass specimens heat treated at 1000°C for 2 h. Devitrification of glass phase has occurred in both Sr-free and Sr-containing glasses due to appearance of intensive peaks in their XRD patterns. However, type of the phases crystallized within the glasses was different to each other. Hydroxyapatite was the main phase in the composition of both Sr-free and Sr-containing specimens, which can be considered Sr-doped hydroxyapatite in Sr-containing specimen, because the XRD patterns of hydroxyapatite (JCPDS: 24–0033) is closely similar to that of Sr-substituted HA (JCPDS: 01-082-1429). The absence or presence of Sr in the glass composition resulted in formation of various calcium silicate phases. In Sr-free specimen calcium silicate was found as α-$CaSiO_3$ (JCPDS: 001-0720). At the presence of Sr, Ca_2SiO_4 phase was identified (JCPDS:029-0369), and the presence of strontium-containing Ca_2SiO_4 such as $CaSrSiO_4$ (JCPDS: 01-0077-1618) and $Ca_{1.8}Sr_{0.2}SiO_4$ (JCPDS: 01-077-1621) is also suggestible, because of the similarity of their individual peaks to that of Ca_2SiO_4 or their overlap with that of apatite phase. The peaks appeared in the pattern of Sr-containing specimen was broader than those appeared in Sr-free one, indicating poor crystallinity of the formed phases in this specimen.

3.2 In vitro bioactivity test

In vitro bioactivity of the glasses was evaluated by soaking the samples in SBF solution and characterizing them by FTIR, XRD and other appropriate techniques.

3.2.1 Concentration of ions released into SBF solution

Figure 4 shows the cumulative concentration of Ca (Fig. 4a), and Si (Fig. 4b) ions released from the samples into the SBF solution. A rapid increase in the Ca concentration occurred during the 2 days for Sr-free and during 4 days for Sr-containing glasses due to higher rate of dissolution process compared with precipitation one. Dissolution rate decreased after 3rd day for Sr-free glass and after 4th day for Sr-glass probably due to formation of apatite layer onto the surfaces of the specimens; however it

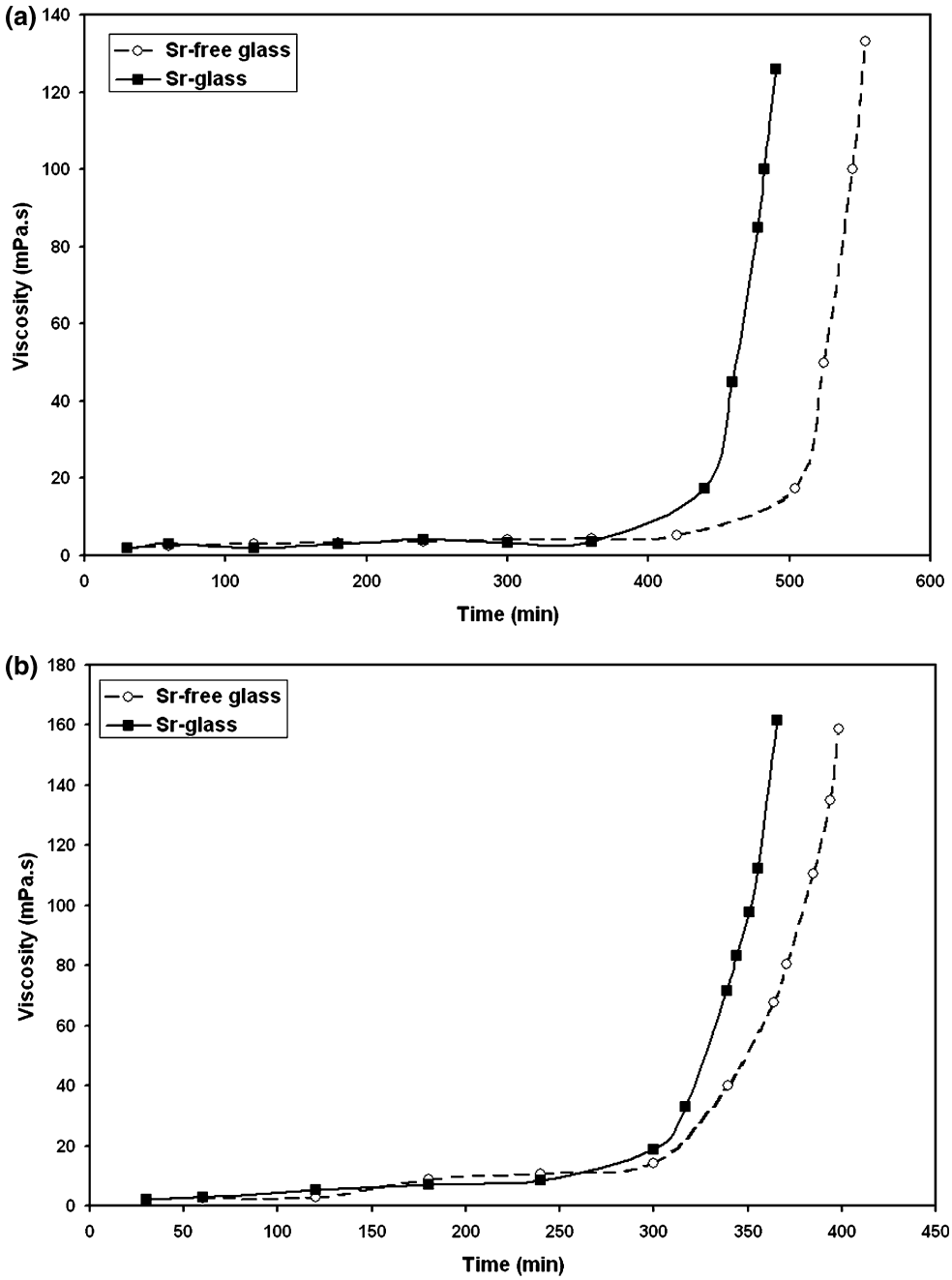

Fig. 1 Viscosity as a function of aging time for Sr-free and Sr-containing bioglasses: **a** T = 25°C, **b** T = 37°C

was still more active than precipitation phenomenon. Decrease in Ca concentration of the solution can be described as follows: once the apatite nuclei are formed, they can grow spontaneously by consuming the calcium and phosphate ions in the surrounding fluid because the body fluid is highly supersaturated with respect to the apatite [25, 26]. Figure 4b shows the cumulative concentration of Si ions of the SBF solution. Rapid release of Si was observed from the glass during the first period of immersion and then a gradual release was observed. Higher solubility of Sr-containing glass in comparison with Sr-free one was confirmed by its higher Si concentration in the SBF solution. It reflects the higher disruption rate of Sr-glass compared to Sr-free glass [27]. This result was in agreement with that of previous studies published on $SrO–CaO–ZnO–SiO_2$ glass ionomer composition [18] and Sr-doped phosphate glasses [19] and suggest that is related to increased disorder of glass network induced by substitution of Ca^{2+} ions by larger ions i.e., Sr^{2+}. The ionic radius of Ca is 1.00°A whereas it is 1.13°A for Sr ion.

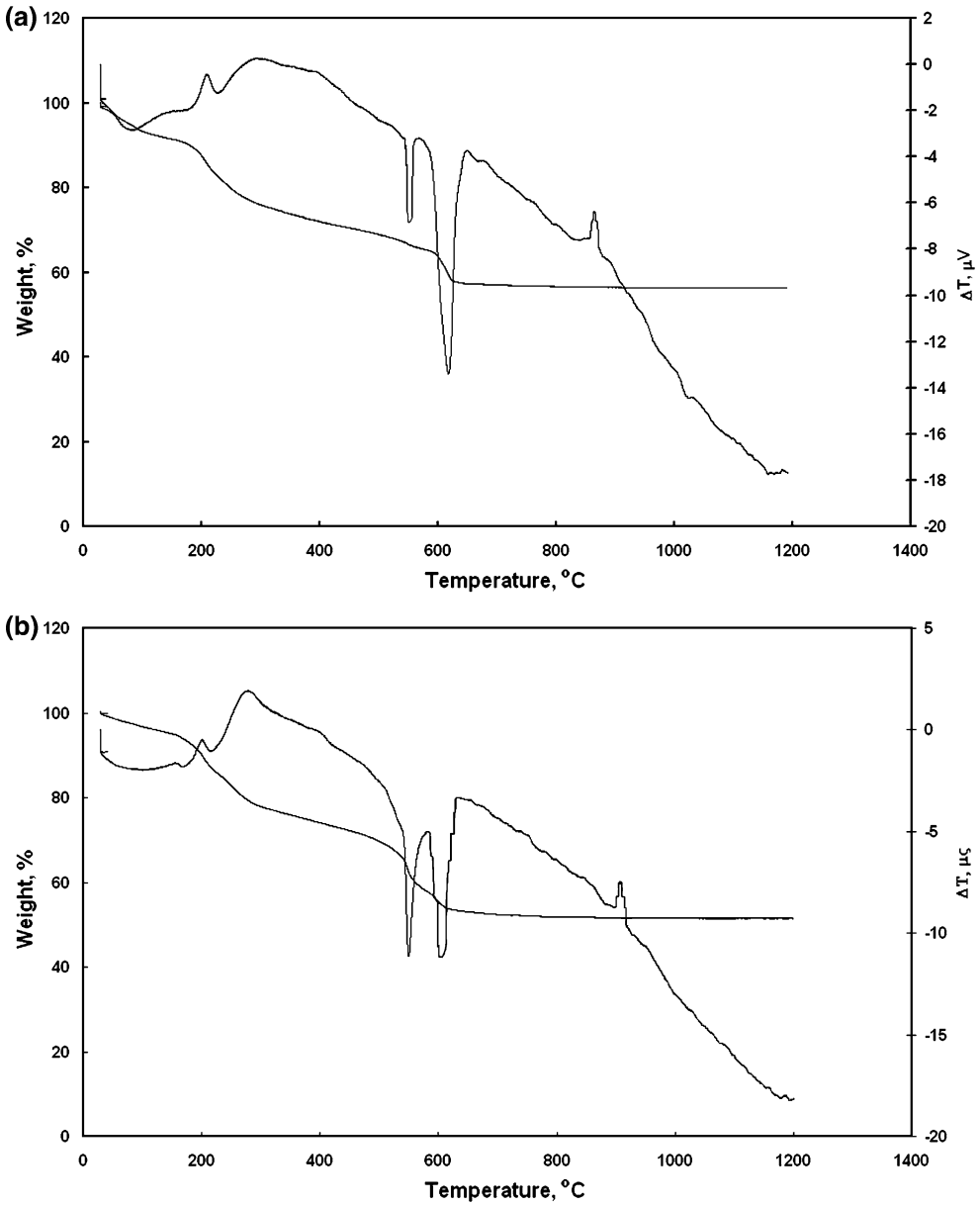

Fig. 2 TG/DTA analysis of sol–gel bioactive glasses: **a** Sr-free and **b** Sr-containing bioglass

3.2.2 XRD

Figure 5 shows the XRD patterns of the Sr-free glass specimen soaked in SBF solution for 1 and 2 weeks. The pattern of the unsoaked specimen is also presented for comparison. Before soaking, the glass exhibited a pattern characteristic of an amorphous structure. Formation of poorly crystalline apatite phase was confirmed by appearance of the broad peaks at $2\theta = 25.9°$ corresponded to (002) planes and $2\theta = 31.8°$ corresponded to (211) atomic planes (standard card no JCPD 24-0033). The XRD patterns of Sr-glass specimen (Fig. 6) was similar to that of Sr-free one but some atomic planes such as (130) ($2\theta = 39.7°$) slightly formed in apatite phase on the surfaces of Sr-free glass did not find here. It has been documented that the presence of some ions such as Mg^{2+} in the bioglass composition inhibits or retards precipitation of calcium phosphate layer [28]. It suggests that Sr ions can also retard calcium phosphate precipitation.

3.2.3 FTIR

Figure 7 shows the FTIR spectra of the glass powders before and after soaking in SBF solution. The FTIR analysis of the stabilized glass (800°C) and the soaked glass of both specimens reveals structural differences assigned

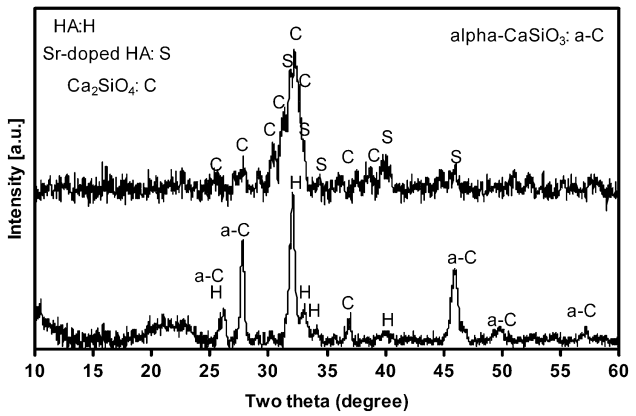

Fig. 3 XRD patterns of bioglass samples after thermal treatment at 1000°C: *Down* Sr-free glass, *upper* Sr-containing glass

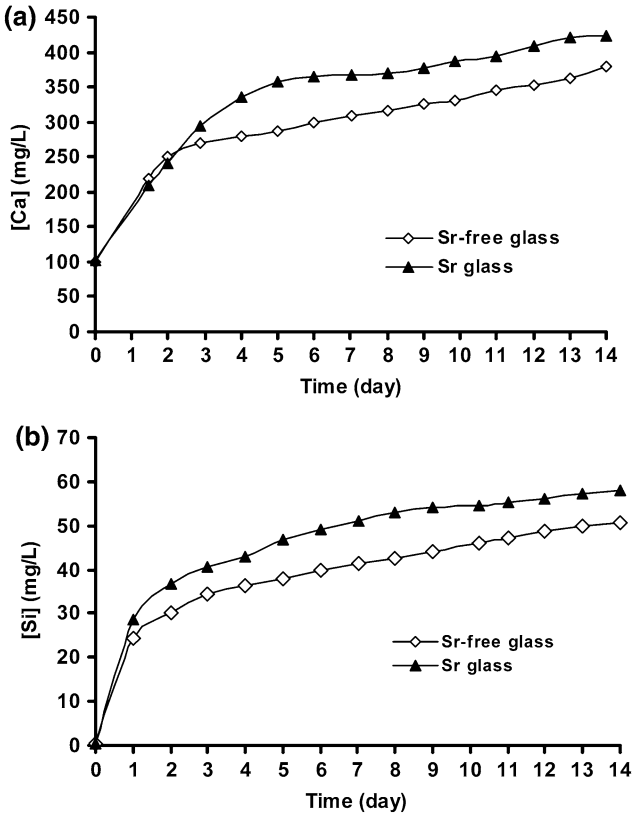

Fig. 4 Cummulative concentration of Ca (**a**) and Si (**b**) released from the glass samples into the SBF solution

to hydroxyl groups (3700 and 3000 cm^{-1}), phosphate groups (570–600 and 1050 cm^{-1}) and Si–O groups (440–450 and 1200–1215 cm^{-1}). The band corresponded to P–O bending vibrations (1050 cm^{-1}) is broader in unsoaked specimens than the immersed one, indicating amorphous nature of the glass before soaking and poor crystallinity of precipitated calcium phosphate after soaking procedure [29]. The absorption bands around 570 and 600 cm^{-1} are also associated with the P–O bending vibrations that are

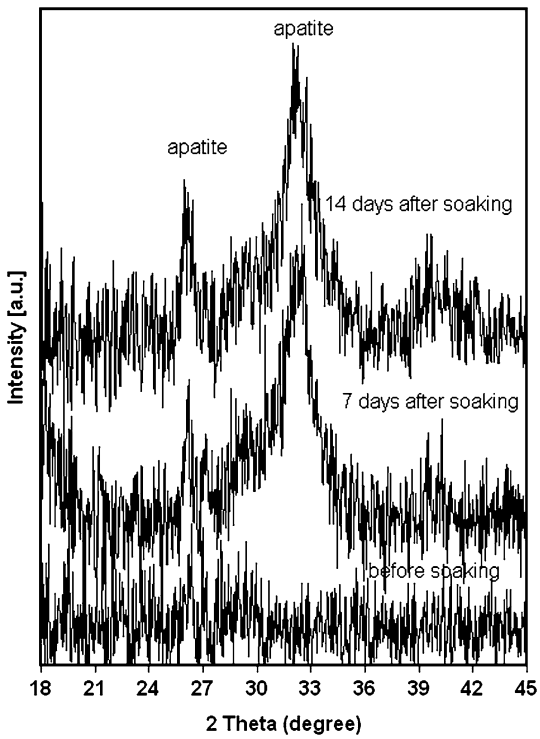

Fig. 5 XRD patterns of Sr-free glass before and after soaking in SBF

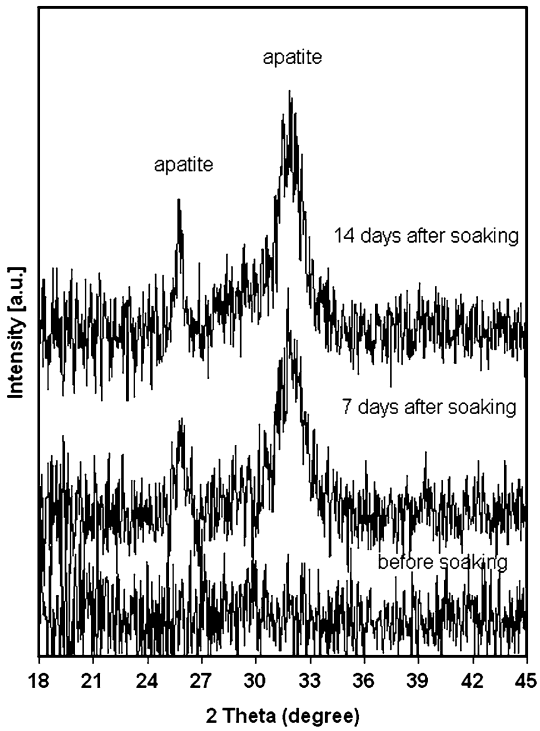

Fig. 6 XRD patterns of Sr-containing glass before and after soaking in SBF

more intensive in the patterns of the soaked samples compared to stabilized ones and indicative of calcium phosphate precipitation [30]. The bands observed at 445,

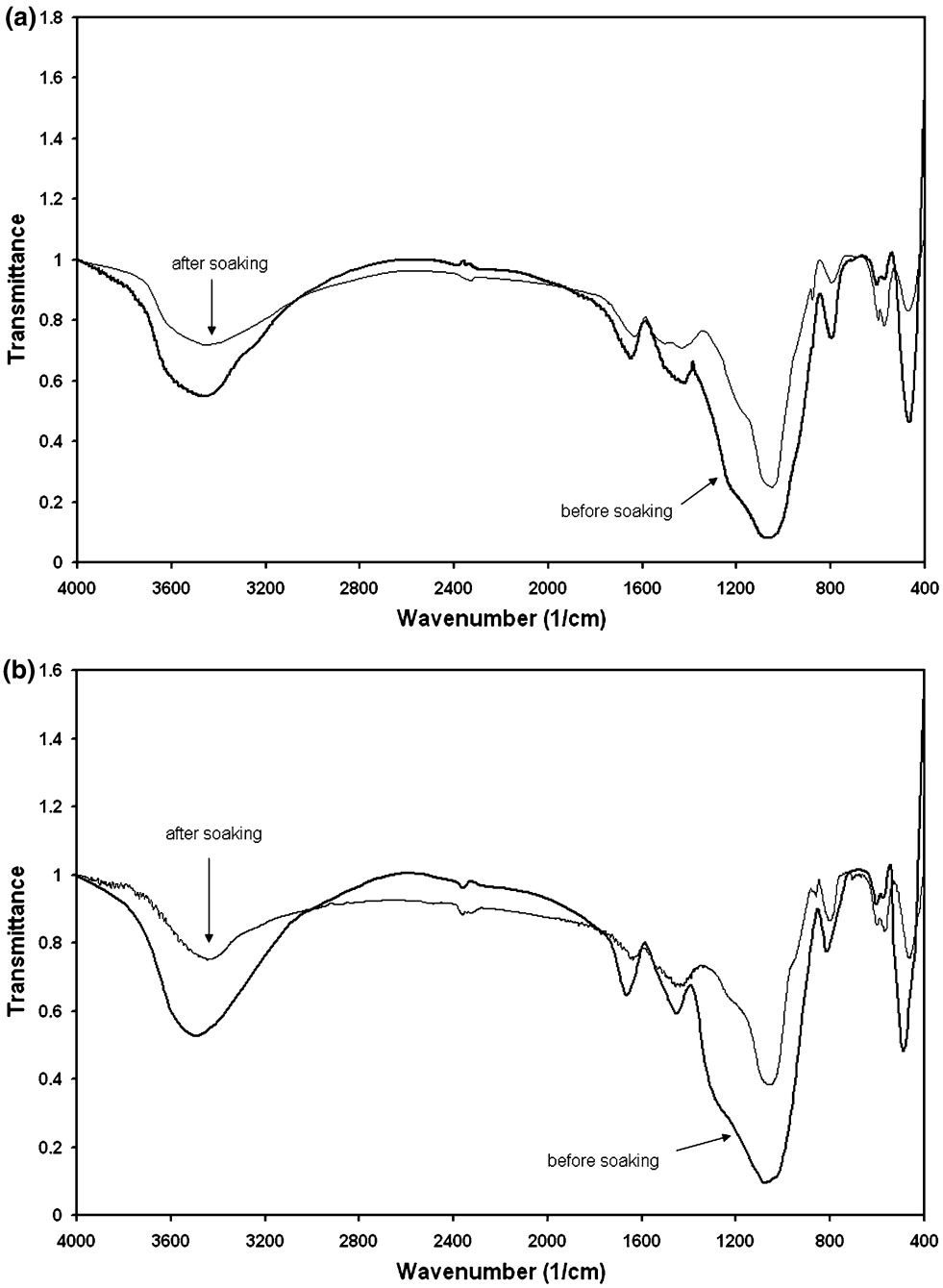

Fig. 7 FTIR spectra of various glasses before and after soaking in SBF: **a** Sr-free glass, **b** Sr-containing glass

800 and 1200 cm^{-1} are attributed to vibration modes of Si–O–Si and their intensities decreased considerably after soaking in SBF solution. Also a right-shift in Si–O–Si vibrations was observed when SrO was introduced into the glass composition which suggest that is related to formation of shortened Si–O–Si bonds in presence of large Sr cations [19]. Furthermore, the bands appeared around 875 and 1422 cm^{-1}, in the spectra of soaked specimens, are assigned to C–O stretching in carbonate groups substituted for phosphate groups in apatite lattice [29]. The latter was resolved in two bands (1422 and 1482 cm^{-1}) in the Sr-free glass, indicating the higher content of carbonate-apatite phase formed on the surfaces of this specimen.

Since surface the layer formed on the glass surfaces was not exactly hydroxyapatite in term of stoichiometry (due to absence of OH band at 630 cm^{-1} and presence of carbonate groups in apatite lattice) it was described by a more general term i.e., calcium phosphates in this study.

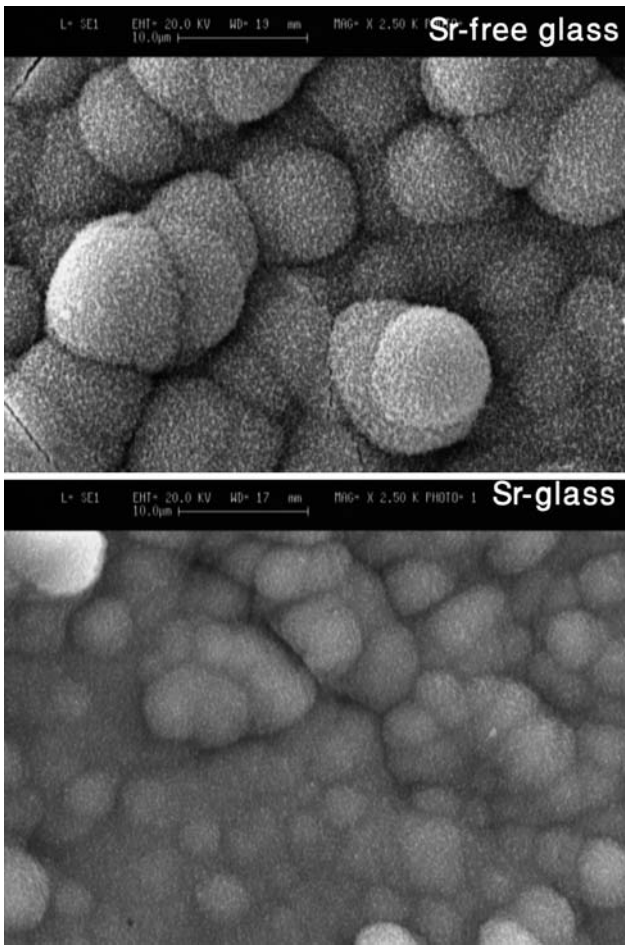

Fig. 8 SEM micrographs of various glasses after soaking in SBF for 7 days

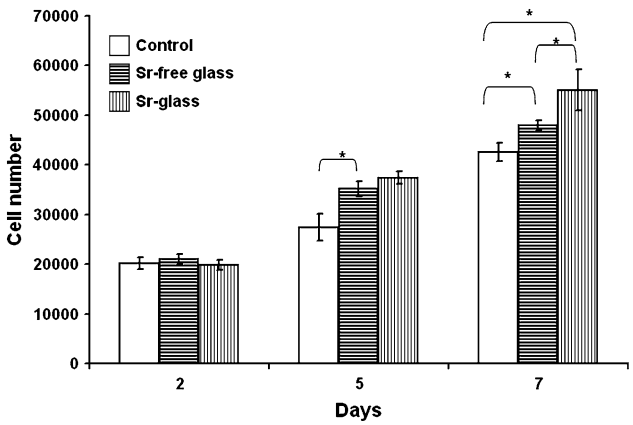

Fig. 9 Proliferation of rat calvaria-derived osteoblastic cells in contact with polystyrene (control), calcium and calcium/strontium silicophosphate glasses (* $P < 0.05$ for n = 4)

3.2.4 SEM observation

Figure 8 shows SEM images from the surfaces of the samples soaked in SBF for 1 week. Ball-like particles covered by a layer of entangled rough crystals were observed in these Figures. It is clear from the pictures that the size of the balls and the roughness of the crystals were higher in Sr-free glass (Fig. 8a) than those in Sr-containing glass (Fig. 8b). It seems that Sr ions limited the growth of calcium phosphate layer.

3.3 Cell proliferation and morphology

Figure 9 shows proliferation of the osteoblastic cells on various specimens measured by MTT assay. After cell attachment, the osteoblasts began a period of proliferation confirmed by the difference of the cell number between days 2, 5 and 7 on all of specimens ($P < 0.05$). At 2nd day, no significant difference in cell proliferation was observed between the control (polystyrene) and the glass specimens ($P \gg 0.05$). At 5th day, the amount of formazon produced by osteoblasts cultured on the glasses was significantly higher than that of polystyrene ($P < 0.05$), meanwhile the difference between the number of cells proliferated on Sr-free glass and Sr-glass was not statistically significant. At 7th day, the number of the cells proliferated on Sr-glass specimen was significantly higher than that of Sr-free glass ($P < 0.05$). The results of this study was in agreement with those of other authors who stated better proliferation of osteoblasts in presence of Sr-containing material [31].Off course, the concentration of the Sr ions in the glass composition may be critical and its higher doses may retard or inhibit cell growth and proliferation, which should be considered in future studies.

Figure 10 shows the morphologies of the osteoblastic cells attached onto the surface of the glass specimens. In both specimens the surface has been covered by polygonal osteoblastic cells with developed cytoplasmic extensions and the cells became confluence on top of the glasses after 7 days.

3.4 ALP activity

Alkaline phosphatase is known as an early osteoblastic differentiation marker [32] and is produced by cells showing mineralized extracellular matrix. ALP activity (Fig. 11) was enhanced from 2nd day to 5th day of culture ($P < 0.01$) and then inhibited on 7th day for all specimens ($P < 0.05$) probably due to conflux of the expanded cells. At day 5th, higher lever of ALP was observed for Sr-glass compared with Sr-free glass ($P < 0.05$). There was no significant difference in ALP activity between polystyrene, Sr-glass and Sr-free glass at 7th day ($P > 0.05$). The results of the cell culture tests of this study suggest better biological performance of sol gel derived Sr-containing bioactive glass in comparison with the Sr-free one.

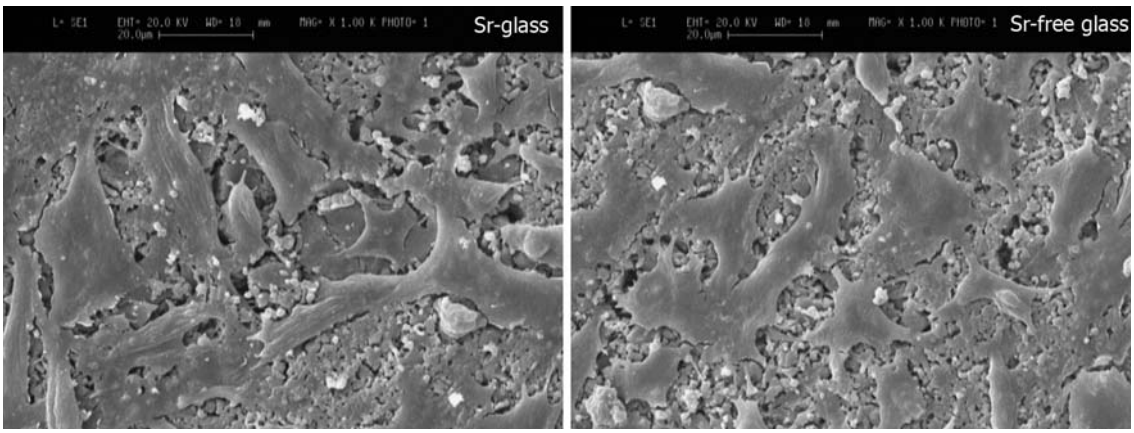

Fig. 10 The morphologies of the osteoblastic cells cultured on pure bioglass specimens. The Cells have attached with normal polygonal

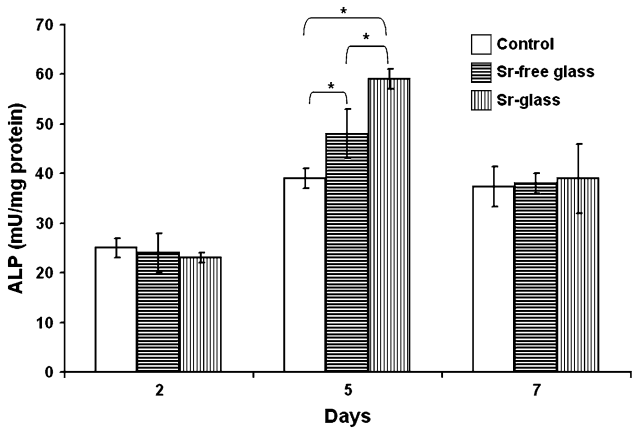

Fig. 11 Alkaline phosphatase activity of rat osteoblastic cells on polystyrene (control), Sr-free and Sr-containing bioactive glasses from 2 to 7 days (* $P < 0.05$, for n = 4)

4 Conclusions

It is concluded from the results that substitution of Sr for Ca in the silicophosphate glass composition can increase the density and glass crystallization temperature and change the type of the crystallized phase. The rate of glass dissolution also increased using SrO in the composition. Formation of apatite phase on the surface of Sr-glass is slightly retarded when soaking it in SBF solution. The glasses produced increased proliferation of rat calvaria osteoblastic cells, meanwhile the use of SrO in the glass composition enhanced the cell proliferation and ALP activity, depending on time parameter.

Acknowledgment The authors gratefully acknowledge Iran National Science Foundation (INSF) for financial support of this work.

References

1. Torricelli P, Fini M, Giavaresi G, Giardino R. In vitro models to test orthopaedic biomaterials in view of their clinical application in osteoporotic bone. Int J Artif Organs. 2004;27:658–63.
2. Moura J, Teixeira LN, Ravagnani C, Peitl O, Zanotto ED, Beloti MM, et al. In vitro osteogenesis on a highly bioactive glass-ceramic (Biosilicate). J Biomed Mater Res A. 2007;82:545–57.
3. Saravanapavan P, Jones JR, Verrier S, Beilby R, Shirtliff VJ, Hench LL, et al. Binary CaO-SiO_2 gel-glasses for biomedical applications. Biomed Mater Eng. 2004;14:467–86.
4. Hench LL. The story of bioglass. J Mater Sci: Mater Med. 2006;17:967–78.
5. Best SM, Porter AE, Thian ES, Huang G. Bioceramics: past, present and for the future. J Eur Ceram Soc. 2008;28:1319–27.
6. Jaroch DB, Clupper DC. Modulation of zinc release from bioactive sol-gel derived SiO_2-CaO-ZnO glasses and ceramics. J Biomed Mater Res A. 2007;82:575–88.
7. Oki A, Parveen B, Hossain S, Adeniji S, Donahue H. Preparation and in vitro bioactivity of zinc containing sol-gel-derived bioglass materials. J Biomed Mater Res A. 2004;69:216–21.
8. Saboori A, Sheikhi M, Moztarzadeh F, Rabiee M, Hesaraki S, Tahriri M, et al. Sol–gel preparation, characterisation and in vitro bioactivity of Mg containing bioactive glass. Adv Apll Ceram. 2009;108:155–61.
9. Balamurugan A, Rebelo AH, Lemos AF, Rocha JH, Ventura JM, Ferreira JM. Suitability evaluation of sol-gel derived Si-substituted hydroxyapatite for dental and maxillofacial applications through in vitro osteoblasts response. Dent Mater. 2008;24:1374–80.
10. Balamurugan A, Balossier G, Kannan S, Michel J, Rebelo AH, Ferreira JM. Development and in vitro characterization of sol-gel derived CaO-P2O5-SiO2-ZnO bioglass. Acta Biomater. 2007;3:255–62.
11. Chen YW, Shi GQ, Ding YL, Yu XX, Zhang XH, Zhao CS, et al. In vitro study on the influence of strontium-doped calcium polyphosphate on the angiogenesis-related behaviors of HUVECs. J Mater Sci Mater Med. 2008;19:2655–62.
12. Canalis E, Hott M, Deloffre P, Tsouderos Y, Marie PJ. The divalent strontium salt S12911 enhances bone cell replication and bone formation in vitro. Bone. 1996;18:517–23.
13. Buehler J, Chappuis P, Saffar JL, Tsouderos Y, Vignery A. Strontium ranelate inhibits bone resorption while maintaining bone formation in alveolar bone in monkeys. Bone. 2001;29:176–9.

14. Hott M, Deloffre P, Tsouderos Y, Marie PJ. S12911–2 reduces bone loss induced by short-term immobilization in rats. Bone. 2003;33:112–23.
15. Meunier PJ, Roux C, Seeman E, Ortolani S, Badurski JE, Spector TD, et al. The effects of strontium ranelate on the risk of vertebral fracture in women with postmenopausal osteoporosis. N Engl J Med. 2004;350:459–568.
16. Seeman E, Devogelaer JP, Lorenc R, Spector T, Brixen K, Balogh A, et al. Strontium ranelate reduces the risk of vertebral fractures in patients with osteopenia. J Bone Miner Res. 2008;23:433–8.
17. Landi E, Tampieri A, Celotti G, Sprio S, Sandri M, Logroscino G. Sr-substituted hydroxyapatites for osteoporotic bone replacement. Acta Biomater. 2007;3:961–9.
18. Boyd D, Towler MR, Watts S, Hill RG, Wren AW, Clarkin OM. The role of Sr2+ on the structure and reactivity of SrO-CaO-ZnO-SiO2 ionomer glasses. J Mater Sci Mater Med. 2008; 19:953–7.
19. Abou Neel EA, Chrzanowski W, Pickup DM, O'Dell LA, Mordan NJ, Newport RJ, et al. Structure and properties of strontium-doped phosphate-based glasses. J R Soc Interface. 2009;6:435–46.
20. Towler M, Boyd D, Freeman C, Brook IM, Farthing P. Comparison of in vitro and in vivo bioactivity of SrO-CaO-ZnO-SiO_2 glass grafts. J Biomater Appl. 2008 (in advance of print).
21. Oréfice RL, Hench LL, Clark AE, Brennan AB. Novel sol-gel bioactive fibers. J Biomed Mater Res. 2001;15(55):460–7.
22. Kokubo T, Kushitani H, Sakka S, Kitsugi T, Yamamuro TJ. Solutions able to reproduce in vivo surface-structure changes in bioactive glass-ceramic A-W. J Biomed Mater Res. 1990;24: 721–34.
23. Neuhoff V, Stamm R, Eibl H. Clear background and highly sensitive protein staining with coomassie blue dyes in polyacrylamide gels: a systematic analysis. Electrophoresis. 1985;6: 427–48.
24. Qiu K, Zhao XJ, Wan CX, Zhao CS, Chen YW. Effect of strontium ions on the growth of ROS17/2.8 cells on porous calcium polyphosphate scaffolds. Biomaterials. 2006;27:1277–86.
25. Neuman W, Neuman M. The chemical dynamics of bone mineral. Chicago: University of Chicago Press; 1958.
26. Gamble J. Chemical anatomy, physiological and pathology of extracellular fluid. Cambridge, MA: Harvard University Press; 1967.
27. Saravanapavan P, Jones JR, Pryce RS, Hench LL. Bioactivity of gel-glass powders in the CaO-SiO2 system: a comparison with ternary (CaO-P2O5-SiO2) and quaternary glasses (SiO2-CaO-P2O5-Na2O). J Biomed Mater Res A. 2003;66:110–9.
28. Roy D. In vitro reactivity of Na_2O-MgO-SiO_2 glasses. J Phys Chem Solid. 2007;68:2321–5.
29. Hesaraki S, Moztarzadeh F, Solati-Hashjin M. Phase evaluation of an effervescent-added apatitic calcium phosphate bone cement. J Biomed Mater Res B (Appl Biomater). 2006;79:203–9.
30. Zhang K, Yan H, Bell DC, Stein A, Francis LF. Effects of materials parameters on mineralization and degradation of sol-gel bioactive glasses with 3D-ordered macroporous structures. J Biomed Mater Res A. 2003;66:860–9.
31. Xue W, Moore JL, Hosick HL, Bose S, Bandyopadhyay A, Lu WW, et al. Osteoprecursor cell response to strontium-containing hydroxyapatite ceramics. J Biomed Mater Res. 2006;79A:804–14.
32. Gotoh Y, Hiraiwa K, Nagayama M. In vitro mineralization of osteoblastic cells derived from human bone. Bone Miner. 1990;8:239–50.